Cell Reports, Volume *42*

Supplemental information

A PINK1 input threshold arises from positive feedback in the PINK1/Parkin mitophagy decision circuit

Christopher S. Waters, Sigurd B. Angenent, Steven J. Altschuler, and Lani F. Wu

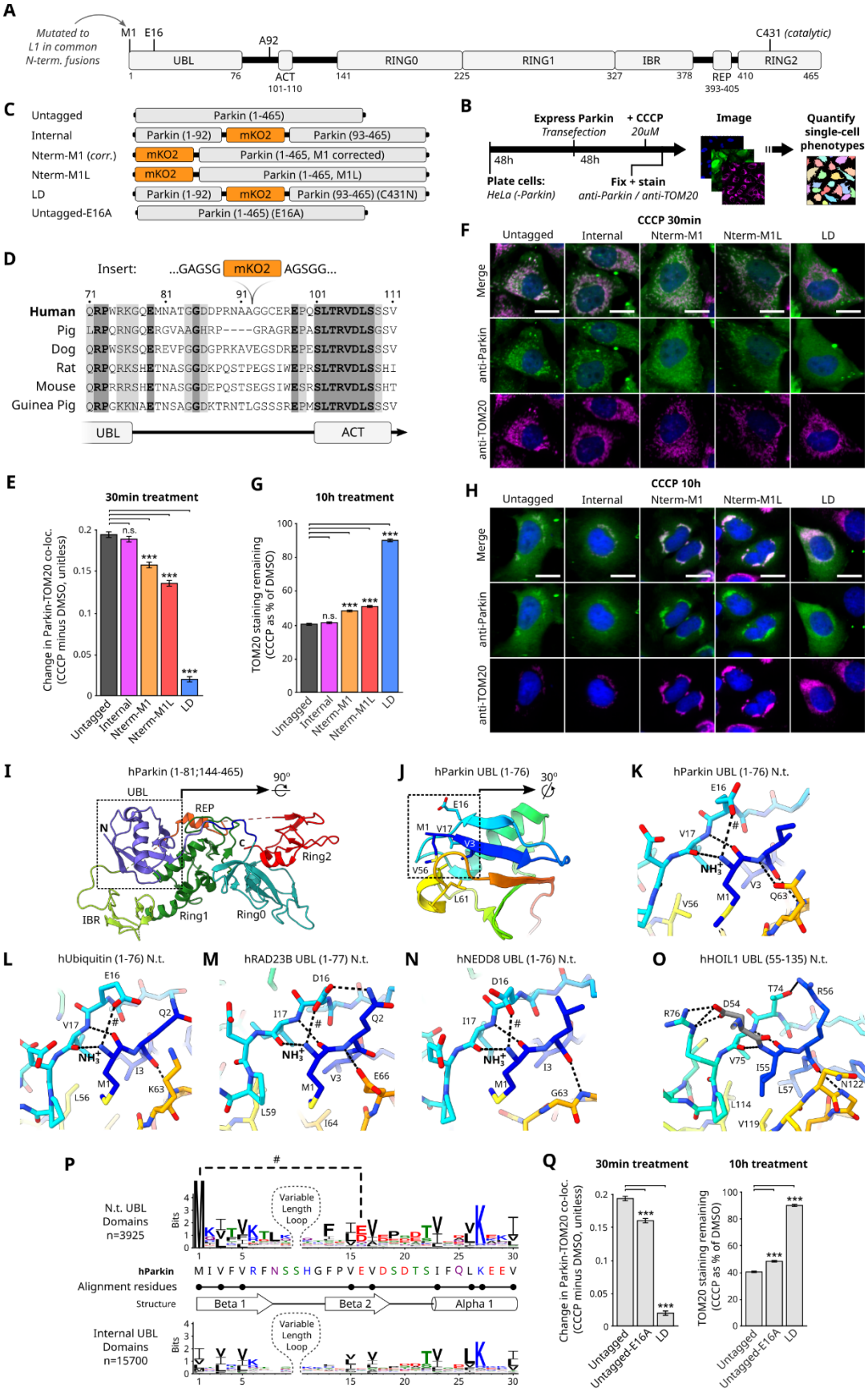
A
Mutated to L1 in common N-term. fusions
M1 E16
A92
C431 (catalytic)
UBL
ACT
RING0
RING1
IBR
REP
RING2
1 76 101-110 141 225 327 378 393-405 410 465
C
Untagged
Parkin (1-465)
Internal
Parkin (1-92) mKO2 Parkin (93-465)
Nterm-M1 (corr.)
mKO2 Parkin (1-465, M1 corrected)
Nterm-M1L
mKO2 Parkin (1-465, M1L)
LD
Parkin (1-92) mKO2 Parkin (93-465) (C431N)
Untagged-E16A
Parkin (1-465) (E16A)
B
Express Parkin Transefection
+ CCCP 20uM
Image
Quantify single-cell phenotypes
48h
48h
Plate cells: HeLa (-Parkin)
Fix + stain anti-Parkin / anti-TOM20
D
Insert: ...GAGSG mKO2 AGSGG...
Human QRPWRKGQEMNATGGDDPRNAAGGCEREPQSLTRVDLSSSV
Pig LRPQRNGQERGVAAGHRP----GRAGREPASLTRVDLSGSV
Dog QRPWSKSQEREVPGGDGPRKAVEGSDREPESLTRVDLSSSV
Rat QRPQRKSHETNASGGDKPQSTPEGSIWEPRSLTRVDLSSHI
Mouse QRPRRRSHETNASGGDEPQSTSEGSIWESRSLTRVDLSSHT
Guinea Pig QRPGKKNAETNSAGGDKTRNTLGSSSREPMSLTRVDLSSSV
UBL ACT
E
30min treatment
Change in Parkin-TOM20 co-loc. (CCCP minus DMSO, unitless)
n.s. *** *** ***
Untagged Internal Nterm-M1 Nterm-M1L LD
G
10h treatment
TOM20 staining remaining (CCCP as % of DMSO)
n.s. *** *** ***
Untagged Internal Nterm-M1 Nterm-M1L LD
F
CCCP 30min
Untagged Internal Nterm-M1 Nterm-M1L LD
Merge
anti-Parkin
anti-TOM20
H
CCCP 10h
Untagged Internal Nterm-M1 Nterm-M1L LD
Merge
anti-Parkin
anti-TOM20
I
hParkin (1-81;144-465)
90°
UBL
REP
N
C
Ring2
IBR
Ring1
Ring0
J
hParkin UBL (1-76)
30°
E16
M1
V17
V3
V56
L61
K
hParkin UBL (1-76) N.t.
E16
V17
#
NH3+
V3
M1
Q63
V56
L
hUbiquitin (1-76) N.t.
E16
V17
Q2
#
NH3+
I3
M1
K63
L56
M
hRAD23B UBL (1-77) N.t.
D16
I17
Q2
#
NH3+
V3
M1
E66
L59
I64
N
hNEDD8 UBL (1-76) N.t.
D16
I17
#
NH3+
I3
M1
G63
O
hHOIL1 UBL (55-135) N.t.
T74
R56
D54
R76
V75
I55
L57
N122
L114
V119
P
N.t. UBL Domains n=3925
#
Variable Length Loop
Bits
hParkin M I V F V R F N S S H G F P V E V D S D T S I F Q L K E E V
Alignment residues
Structure
Beta 1 Beta 2 Alpha 1
Internal UBL Domains n=15700
Variable Length Loop
Bits
Q
30min treatment
Change in Parkin-TOM20 co-loc. (CCCP minus DMSO, unitless)
*** ***
Untagged Untagged-E16A LD
10h treatment
TOM20 staining remaining (CCCP as % of DMSO)
*** ***
Untagged Untagged-E16A LD

Figure S1. Identification of an internal Parkin tagging site that preserves function, related to Figure 1. (A) Parkin domain map. UBL: ubiquitin-like. ACT: activating. REP: repressive. Four RING-like domains: RING0, RING1, IBR (in between RING), and RING2. Selected residues marked. M1 indicates Parkin's N-terminal methionine. **(B)** Immunofluorescence (IF) approach for assessing Parkin function. HeLa cells lack endogenous Parkin expression. Parkin expressed by transient transfection (methods). Anti-TOM20 stains mitochondria. Bar length not to scale. **(C)** Parkin fusion proteins, assessed for activity. M1L mutation was carried over from the mCherry-Parkin cloning source and was corrected to make Nterm-M1(corr.). LD: ligase dead **(D)** Conservation of residues at Parkin's internal tagging site. **(E)** Change in Parkin localization due to CCCP treatment (methods). Co-localization (Co-loc.), intensity correlation (Pearson; methods). Mean, 95% confidence intervals, and statistical significance calculated by bootstrap analysis (B=10,000). Bonferroni multiple comparison adjustment. ***$p<0.001$; n.s.: not significant. **(F)** Representative images showing Parkin recruitment. Scale bars: 20um. **(G)** Mean TOM20 depletion due to CCCP treatment. Bootstrap approach as in (E). AFU, arbitrary fluorescence units. **(H)** Representative images showing TOM20 loss. Scale bars: 20um. **(I-K)** Human Parkin structure (PDB: 5C1Z). **(I)** Full protein. **(J)** UBL domain. **(K)** N-terminus (N.t.) of UBL domain. Carbon: color gradient. Oxygen: red. Nitrogen: blue. Sulfur, yellow. Dotted lines: predicted interactions. #: predicted salt bridge between E16 and the N.t. NH_3^+ which would be disrupted by any N-terminal tag. **(L-N)** N.t. structures of human Ubiquitin and other N.t. UBL domains (PDB: 1F9J, 1UEL, and 1NDD respectively). **(O)** N.t. structure of human HOIL1's internal UBL domain (PDB: 2LGY). N.t. of ubiquitin fold stabilized by additional interactions involving D54. Gray coloring: N-terminal extension to canonical UBL fold. **(P)** Sequence logo showing amino acid conservation in UBL domains. Analysis across unique UBL domains in the Uniprot database (methods). Residues used for motif-based alignment are marked (methods). **(Q)** E16A Parkin mutant phenocopies functional defect of N-terminal tags. Functional evaluation as in (E-G).

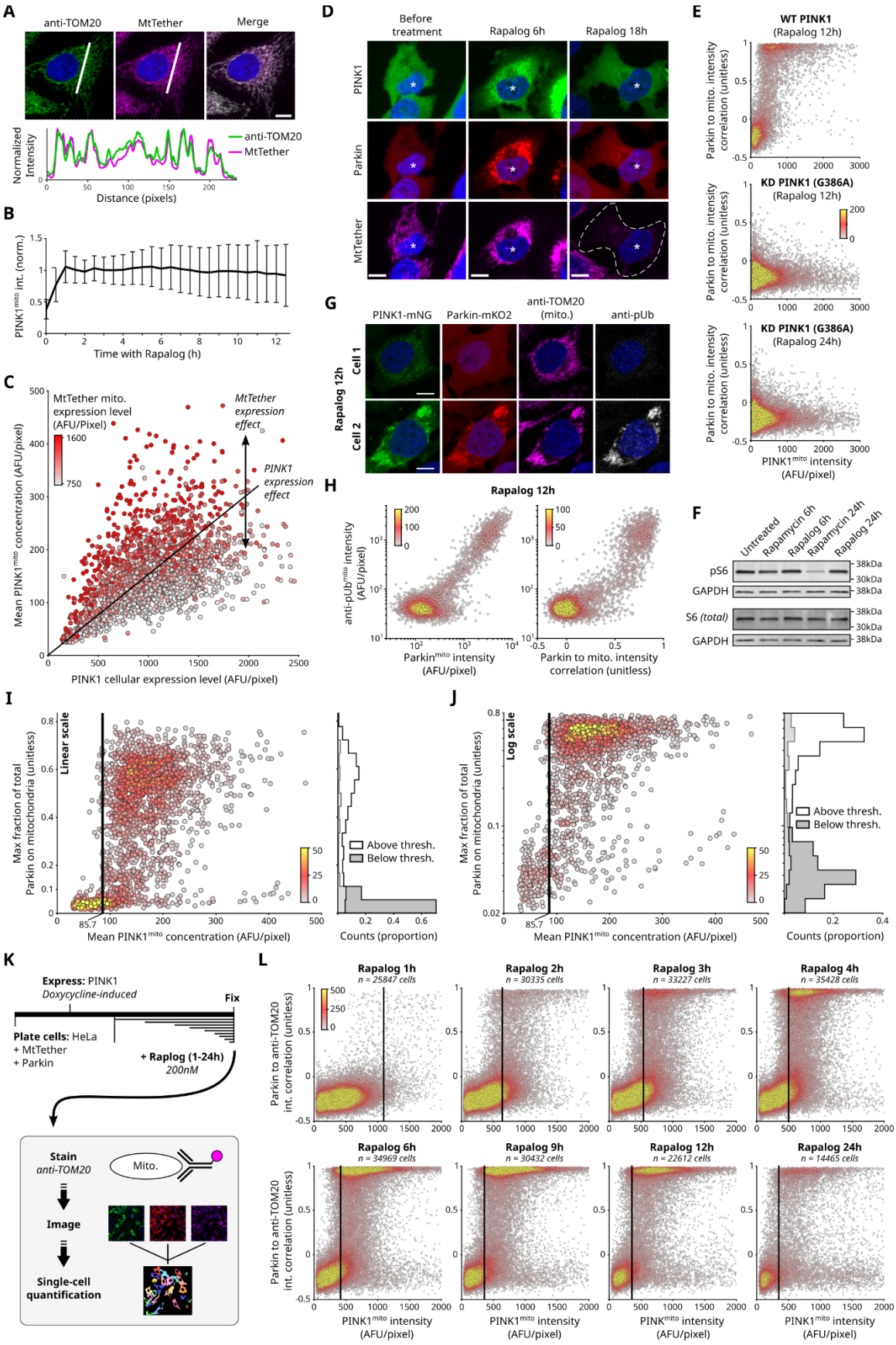
A
anti-TOM20
MtTether
Merge
Normalized Intensity
anti-TOM20
MtTether
Distance (pixels)
B
PINK1mito int. (norm.)
Time with Rapalog (h)
C
MtTether mito. expression level (AFU/Pixel)
1600
750
MtTether expression effect
PINK1 expression effect
Mean PINK1mito concentration (AFU/pixel)
PINK1 cellular expression level (AFU/pixel)
D
Before treatment
Rapalog 6h
Rapalog 18h
PINK1
Parkin
MtTether
E
WT PINK1 (Rapalog 12h)
KD PINK1 (G386A) (Rapalog 12h)
KD PINK1 (G386A) (Rapalog 24h)
Parkin to mito. intensity correlation (unitless)
PINK1mito intensity (AFU/pixel)
G
PINK1-mNG
Parkin-mKO2
anti-TOM20 (mito.)
anti-pUb
Rapalog 12h
Cell 1
Cell 2
H
Rapalog 12h
anti-pUbmito intensity (AFU/pixel)
Parkinmito intensity (AFU/pixel)
Parkin to mito. intensity correlation (unitless)
F
Untreated
Rapamycin 6h
Rapalog 6h
Rapamycin 24h
Rapalog 24h
pS6
GAPDH
S6 (total)
GAPDH
38kDa
30kDa
I
Linear scale
Max fraction of total Parkin on mitochondria (unitless)
Mean PINK1mito concentration (AFU/pixel)
Above thresh.
Below thresh.
Counts (proportion)
J
Log scale
Max fraction of total Parkin on mitochondria (unitless)
Mean PINK1mito concentration (AFU/pixel)
Above thresh.
Below thresh.
Counts (proportion)
K
Express: PINK1
Doxycycline-induced
Fix
Plate cells: HeLa
+ MtTether
+ Parkin
+ Raplog (1-24h)
200nM
Stain
anti-TOM20
Mito.
Image
Single-cell quantification
L
Rapalog 1h
n = 25847 cells
Rapalog 2h
n = 30335 cells
Rapalog 3h
n = 33227 cells
Rapalog 4h
n = 35428 cells
Rapalog 6h
n = 34969 cells
Rapalog 9h
n = 30432 cells
Rapalog 12h
n = 22612 cells
Rapalog 24h
n = 14465 cells
Parkin to anti-TOM20 int. correlation (unitless)
PINK1mito intensity (AFU/pixel)

Figure S2. Characterization of the PINK1/Parkin synthetic circuit, related to Figure 1 and 2. (A) MtTether localization matches that of mitochondrial protein TOM20. Top: Representative images. Bottom: pixel intensities along white lines in images. Scale bar: 20um. **(B)** Average $PINK1^{mito}$ levels are relatively stable over time. Mean and standard deviation, per imaging timepoint, across 1987 normalized cell traces (methods). **(C)** Relationship between $PINK1^{mito}$ and cellular expression of PINK1 and MtTether. Points: 1987 individual cells, colored by MtTether expression level. Lines: empirical trends **(D)** Representative live-cell imaging of mitochondrial loss following prolonged rapalog-driven $PINK1^{mito}$ and $Parkin^{mito}$ recruitment. Asterisk: cell of interest. Dotted line: cell boundary. Scale bars: 10um. **(E)** Kinase dead (KD) PINK1 (G386A) is not capable of recruiting Parkin. Points: single-cell measurements of fixed cells, colored by local point density. **(F)** Effect of rapalog treatment on mTOR signaling (pS6; methods). Rapamycin: positive control, 100nM. Rapalog: 200nM. **(G-H)** $Parkin^{mito}$ recruitment correlated with pUb^{mito} levels. **(G)** Representative images of two cells: with or without anti-pUb^{mito} staining and $Parkin^{mito}$ fluorescence. Scale bars: 10um. **(H)** Fixed cell analysis and comparison of anti-pUb staining. Left: linear correlation between amounts of pUb^{mito} and $Parkin^{mito}$. Right: $Parkin^{mito}$ intensity correlation detects $Parkin^{mito}$ recruitment before pUb^{mito} levels detectably rise. Points: single-cell measurements of fixed cells, colored by local point density. **(I-J)** Re-analysis of circuit input and response from Fig. 2A for alternative response metric: max fraction of Parkin on mitochondria. Vertical line, re-calculated PINK1 input threshold (methods). Points, 1987 individual cells, colored by local point density. Y-axis shown with linear (I) and log (J) scales for clearer visualization. **(K-L)** Measurement of the PINK1/Parkin synthetic circuit behavior using fixed cell analysis. **(K)** Experimental approach. Bar length not to scale. **(L)** Single-cell $Parkin^{mito}$ localization versus $PINK1^{mito}$ concentration at various rapalog treatment durations. Points: single-cell measurements of fixed cells, colored by local point density, pooled from three experimental replicates. Vertical lines, $PINK^{mito}$ concentration for cells undergoing $Parkin^{mito}$ recruitment (methods). Progressive datapoint scarcity caused by mitochondrial degradation.

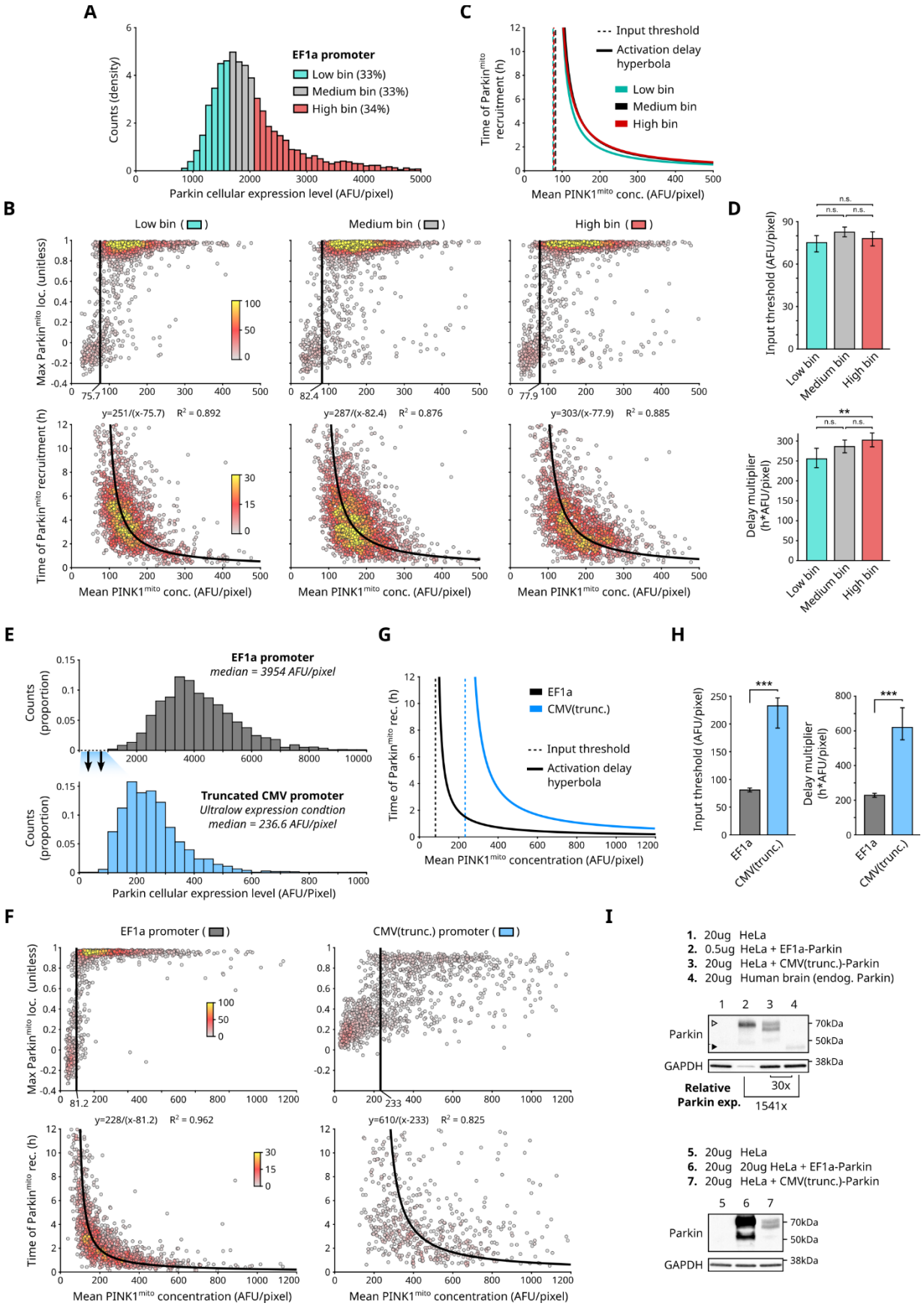
A
EF1a promoter
Low bin (33%)
Medium bin (33%)
High bin (34%)
Counts (density)
Parkin cellular expression level (AFU/pixel)
C
Input threshold
Activation delay hyperbola
Low bin
Medium bin
High bin
Time of Parkin^mito recruitment (h)
Mean PINK1^mito conc. (AFU/pixel)
B
Low bin
Medium bin
High bin
Max Parkin^mito loc. (unitless)
75.7
82.4
77.9
y=251/(x-75.7) R² = 0.892
y=287/(x-82.4) R² = 0.876
y=303/(x-77.9) R² = 0.885
Time of Parkin^mito recruitment (h)
Mean PINK1^mito conc. (AFU/pixel)
D
Input threshold (AFU/pixel)
Delay multiplier (h*AFU/pixel)
n.s.
**
Low bin
Medium bin
High bin
E
EF1a promoter
median = 3954 AFU/pixel
Truncated CMV promoter
Ultralow expression condtion
median = 236.6 AFU/pixel
Counts (proportion)
Parkin cellular expression level (AFU/Pixel)
G
EF1a
CMV(trunc.)
Input threshold
Activation delay hyperbola
Time of Parkin^mito rec. (h)
Mean PINK1^mito concentration (AFU/pixel)
H
***
Input threshold (AFU/pixel)
Delay multiplier (h*AFU/pixel)
EF1a
CMV(trunc.)
F
EF1a promoter
CMV(trunc.) promoter
Max Parkin^mito loc. (unitless)
81.2
233
y=228/(x-81.2) R² = 0.962
y=610/(x-233) R² = 0.825
Time of Parkin^mito rec. (h)
Mean PINK1^mito concentration (AFU/pixel)
I
1. 20ug HeLa
2. 0.5ug HeLa + EF1a-Parkin
3. 20ug HeLa + CMV(trunc.)-Parkin
4. 20ug Human brain (endog. Parkin)
1 2 3 4
Parkin
GAPDH
70kDa
50kDa
38kDa
Relative Parkin exp.
30x
1541x
5. 20ug HeLa
6. 20ug 20ug HeLa + EF1a-Parkin
7. 20ug HeLa + CMV(trunc.)-Parkin
5 6 7
Parkin
GAPDH
70kDa
50kDa
38kDa

Figure S3. Effect of Parkin expression on PINK1/Parkin synthetic circuit dynamics, related to Figure 2. (A-D) The effect of Parkin expression levels on synthetic circuit behavior. **(A)** Distribution of single-cell Parkin expression levels, from the synthetic circuit's standard EF1a promoter, split into three equally sized groups (percentage of total noted). Live-cell data from four experiments was pooled. Counts normalized to bin width (density). **(B)** Quantification of PINK1 input threshold (top) and reciprocal activation delay hyperbola (bottom) for cells in expression groups in (A). Points: individual cells, colored by local point density. **(C)** Threshold and hyperbolas from (B), overlaid. **(D)** Bootstrap statistical analysis of input threshold and delay scaler values for data in (B-C). Mean, 95% confidence intervals, and statistical significance calculated by bootstrap analysis (B=10,000). Bonferroni multiple comparison adjustment. **p<0.01; n.s.: not significant. **(E-H)** Circuit behaviors preserved at ultralow Parkin expression levels. **(E)** Ultralow Parkin expression driven by a truncated CMV promoter, CMV(trunc.), compared to that of the EF1a promoter, measured by fluorescence microscopy. Values for EF1a promoter differ from (A) due to longer exposure times required to image CMV(trunc.) condition. **(F)** Quantification of circuit behaviors for expression conditions in (E) from live cells. Increased noise in the CMV(trunc.) from Parkin expression approaching instrument's background fluorescence levels. **(G)** Threshold and hyperbolas from (F), overlaid. **(H)** Bootstrap statistical analysis of input threshold and delay scaler values for data in (F-G). Mean, 95% confidence intervals, and statistical significance calculated by bootstrap analysis (B=10,000). Bonferroni multiple comparison adjustment. ***p<0.001. **(I)** Characterization of Parkin expression levels compared to that of endogenous Parkin in human brain lysate. Amount of loaded protein is listed for each lane. Filled/empty triangles indicate endogenous/mKO2-tagged Parkin respectively. Band intensity quantification shown for lane 2 and 3 normalized to GAPDH and compared to lane 4 (methods). Fold difference of expression between EF1a and CMV(trunc.) differs from (E) due to effect of background fluorescence in CMV(trunc.) condition. Double band in lane 3 may indicate presence of truncated protein. Decreased protein function due to truncation may contribute to increased threshold and delay in (F-H) causing overestimation of the repressive effect of ultralow Parkin expression.

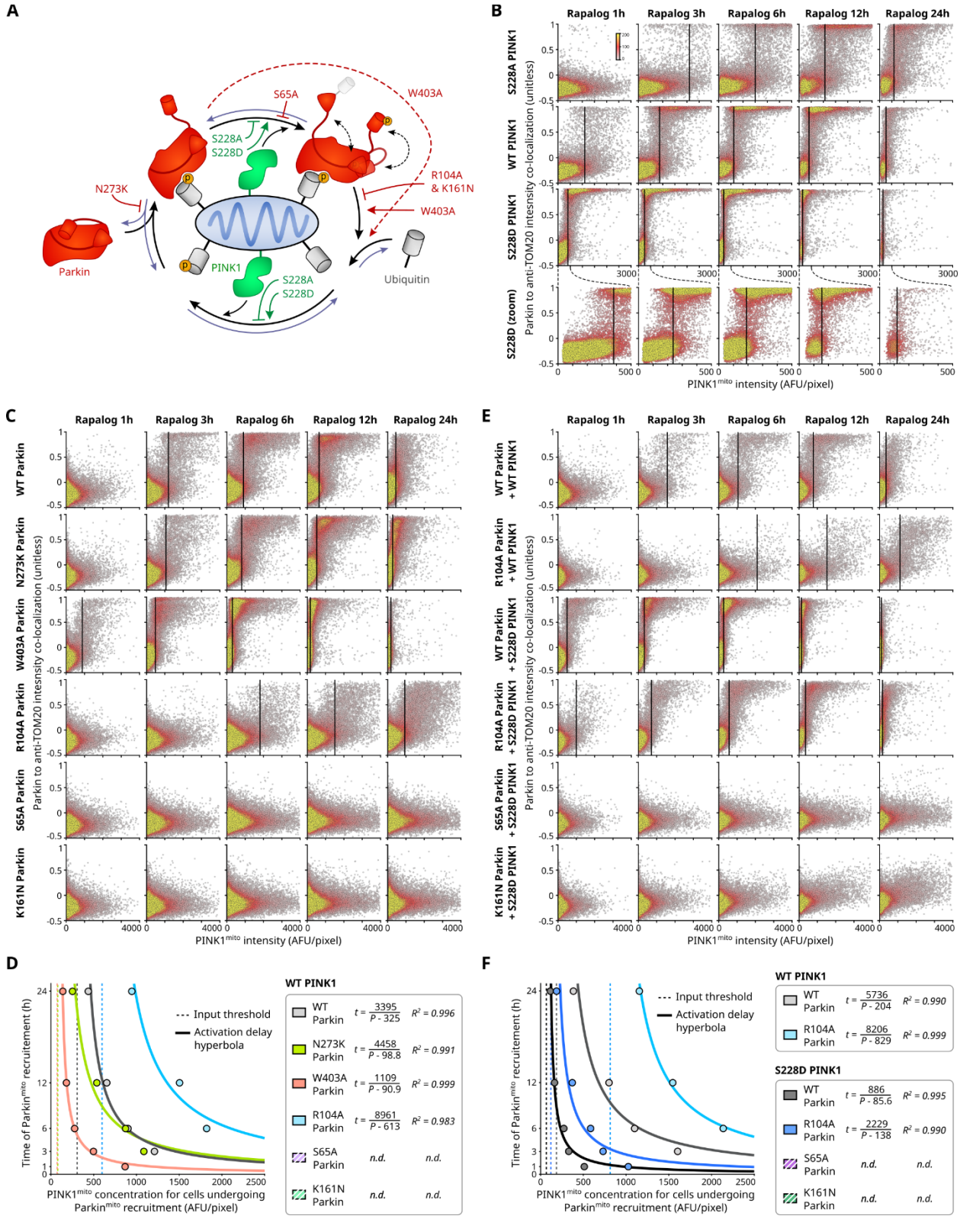
A
S65A
W403A
S228A
S228D
R104A
& K161N
N273K
W403A
Parkin
PINK1
S228A
S228D
Ubiquitin
B
Rapalog 1h
Rapalog 3h
Rapalog 6h
Rapalog 12h
Rapalog 24h
S228A PINK1
WT PINK1
S228D PINK1
S228D (zoom)
Parkin to anti-TOM20 intesnsity co-localization (unitless)
PINK1mito intensity (AFU/pixel)
C
WT Parkin
N273K Parkin
W403A Parkin
R104A Parkin
S65A Parkin
K161N Parkin
Parkin to anti-TOM20 intesnsity co-localization (unitless)
PINK1mito intensity (AFU/pixel)
E
WT Parkin + WT PINK1
R104A Parkin + WT PINK1
WT Parkin + S228D PINK1
R104A Parkin + S228D PINK1
S65A Parkin + S228D PINK1
K161N Parkin + S228D PINK1
Parkin to anti-TOM20 intesnsity co-localization (unitless)
PINK1mito intensity (AFU/pixel)
D
Time of Parkinmito recruitement (h)
Input threshold
Activation delay hyperbola
PINK1mito concentration for cells undergoing Parkinmito recruitment (AFU/pixel)
WT PINK1
WT Parkin t = 3395 / P - 325 R² = 0.996
N273K Parkin t = 4458 / P - 98.8 R² = 0.991
W403A Parkin t = 1109 / P - 90.9 R² = 0.999
R104A Parkin t = 8961 / P - 613 R² = 0.983
S65A Parkin n.d. n.d.
K161N Parkin n.d. n.d.
F
Time of Parkinmito recruitement (h)
Input threshold
Activation delay hyperbola
PINK1mito concentration for cells undergoing Parkinmito recruitment (AFU/pixel)
WT PINK1
WT Parkin t = 5736 / P - 204 R² = 0.990
R104A Parkin t = 8206 / P - 829 R² = 0.999
S228D PINK1
WT Parkin t = 886 / P - 85.6 R² = 0.995
R104A Parkin t = 2229 / P - 138 R² = 0.990
S65A Parkin n.d. n.d.
K161N Parkin n.d. n.d.

Figure S4. Single-cell data for evaluating behavior of PINK1 and Parkin mutants, related to Figure 3 and 4. (A) PINK1 (green) and Parkin (red) mutation effects in full circuit context. Mutation arrows/T-bars: enhancement/repression (resp.). All affects are modulatory, except for S65A which completely blocks Parkin phosphorylation by PINK1. Relative strength of W403A bypass is unknown. **(B)** Single-cell source data for Fig. 3C-D. Points: single-cell measurements of fixed cells, colored by local point density. Single-cell data pooled from two plate replicates. Vertical black lines: estimated $PINK1^{mito}$ concentration of cells undergoing $Parkin^{mito}$ recruitment (methods). Progressive datapoint scarcity caused by mitochondrial degradation. Bottom row: rescaled x-axis for clearer visualization. **(C)** Single-cell source data for Fig. 4C. Representation and analysis as in (B). Single-cell data pooled from two experimental replicates of three plate replicates each. **(D)** Effect of Parkin mutations on PINK1 circuit behavior. Points: aggregate quantification from fixed cell measurements in (C). n.d.: not determined due to lack of $Parkin^{mito}$ recruitment. **(E-F)** Single-cell source data for Fig. 4D. Representation and analysis as in (C-D). Single-cell data pooled from two experimental replicates of three plate replicates each.

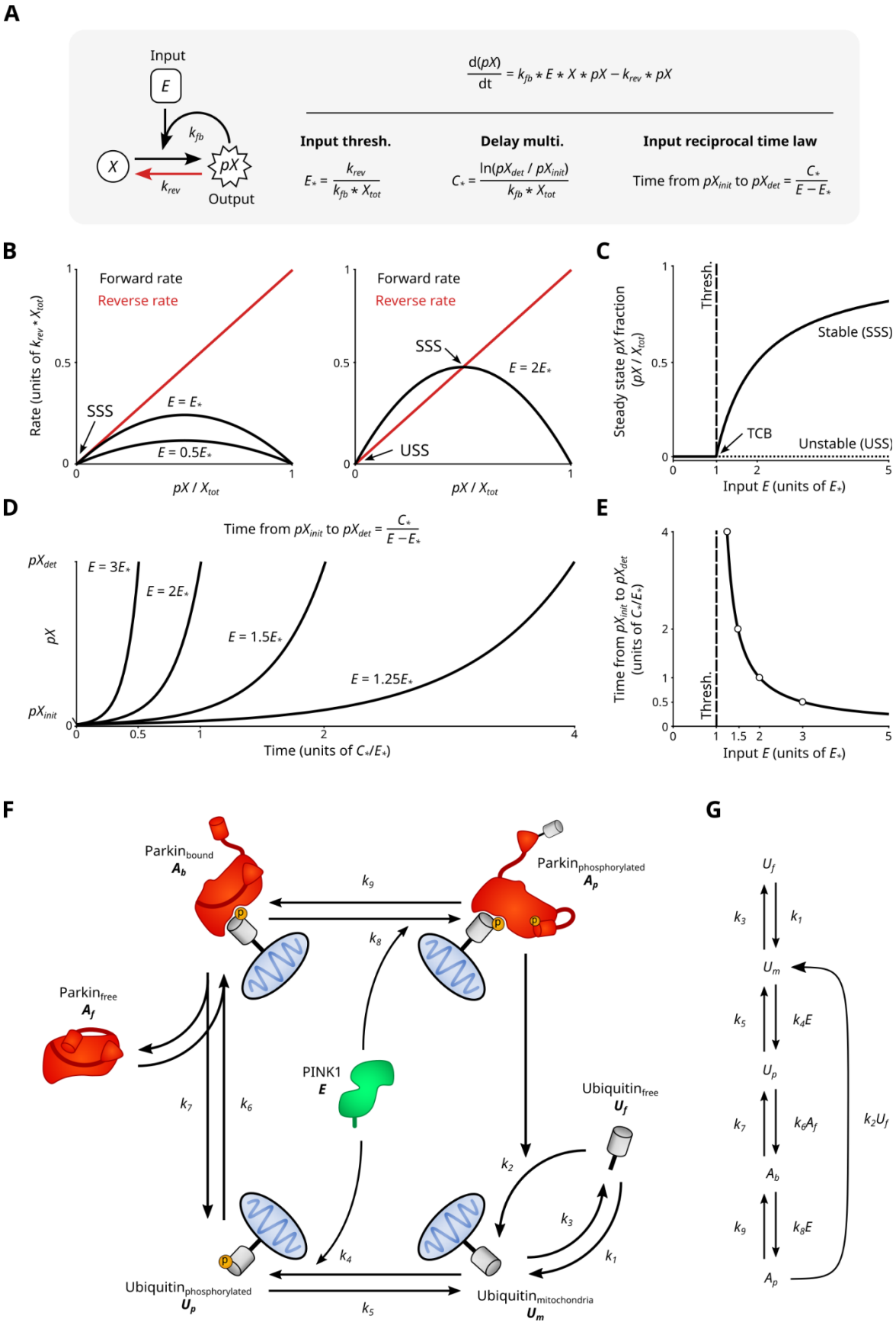
A
Input
E
X
pX
Output
k_{fb}
k_{rev}
$\frac{d(pX)}{dt} = k_{fb} * E * X * pX - k_{rev} * pX$
Input thresh.
$E_* = \frac{k_{rev}}{k_{fb} * X_{tot}}$
Delay multi.
$C_* = \frac{\ln(pX_{det} / pX_{init})}{k_{fb} * X_{tot}}$
Input reciprocal time law
Time from pX_{init} to $pX_{det} = \frac{C_*}{E - E_*}$
B
Forward rate
Reverse rate
SSS
$E = E_*$
$E = 0.5E_*$
Rate (units of $k_{rev} * X_{tot}$)
pX / X_{tot}
Forward rate
Reverse rate
SSS
$E = 2E_*$
USS
pX / X_{tot}
C
Thresh.
Stable (SSS)
TCB
Unstable (USS)
Steady state pX fraction (pX / X_{tot})
Input E (units of E_*)
D
Time from pX_{init} to $pX_{det} = \frac{C_*}{E - E_*}$
pX_{det}
pX
pX_{init}
$E = 3E_*$
$E = 2E_*$
$E = 1.5E_*$
$E = 1.25E_*$
Time (units of C_*/E_*)
E
Thresh.
Time from pX_{init} to pX_{det} (units of C_*/E_*)
Input E (units of E_*)
F
Parkin$_{bound}$ A_b
Parkin$_{phosphorylated}$ A_p
Parkin$_{free}$ A_f
PINK1 E
Ubiquitin$_{free}$ U_f
Ubiquitin$_{phosphorylated}$ U_p
Ubiquitin$_{mitochondria}$ U_m
k_1
k_2
k_3
k_4
k_5
k_6
k_7
k_8
k_9
G
U_f
U_m
U_p
A_b
A_p
k_1
k_3
k_4E
k_5
k_6A_f
k_7
k_8E
k_9
k_2U_f

Figure S5. Input-coupled positive feedback produces threshold and reciprocal activation delay behavior, related to Figure 5. (A) Rate equations for minimal model of input-coupled positive feedback circuit as in Fig. 5A. Parameters E_* and C_* govern input threshold and reciprocal activation delay, respectively. **(B)** Rate analyses for example values of E below or above the input threshold. Forward ($k_{fb} * E * X * pX$) and reverse ($k_{rev} * pX$) reaction rates are plotted (methods). Stable steady states (SSS) and unstable steady states (USS) are identified. **(C)** Steady state analysis illustrating the system's transcritical bifurcation (TCB) that defines the input threshold (methods). For input, *E,* levels below the TCB, the system has one stable steady. For input, *E,* values above the TCB, the system has two stable states, one stable and one unstable (B, right). **(D)** Exponential growth of pX from pX_{init} to pX_{det} for various values of E (methods). Equation describing hyperbolic relationship between E and time to reach pX_{det} is shown. **(E)** Relationship between E and time to reach pX_{det} (methods). Examples from (F), marked with empty circles. **(F)** Parameterized more complete model of the PINK1/Parkin circuit. Variables are defined: Parkin, A; Ubiquitin, U; PINK1, E. Numbered rate constants "k_i" are indexed by step. **(G)** Simple schematic of the model. Rate of each step obtained by multiplying the source moiety (e.g. U_f) by the rate shown (e.g. k_1).

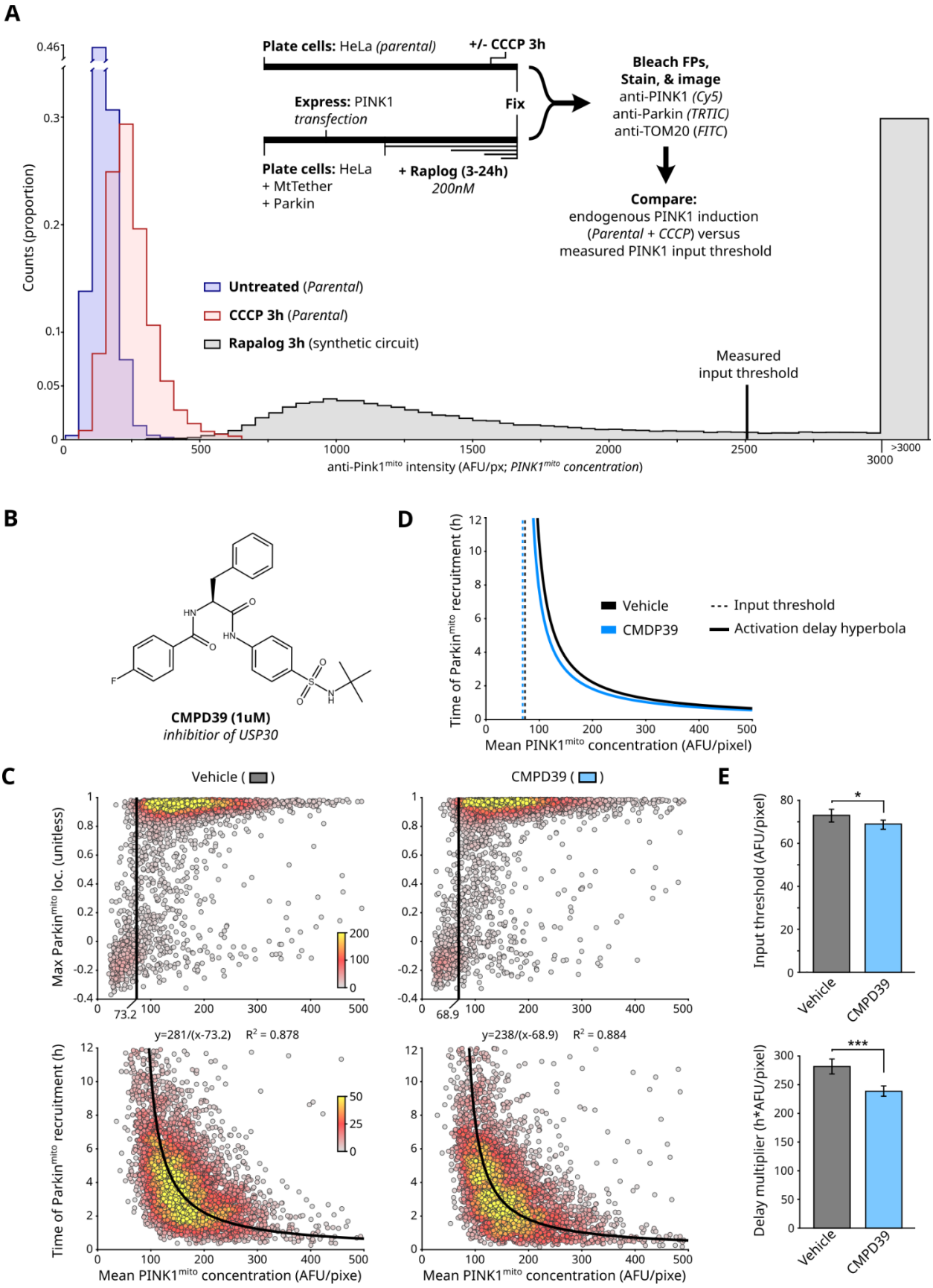
A
Plate cells: HeLa (parental)
+/- CCCP 3h
Express: PINK1
transfection
Fix
Plate cells: HeLa
+ MtTether
+ Parkin
+ Raplog (3-24h)
200nM
Bleach FPs,
Stain, & image
anti-PINK1 (Cy5)
anti-Parkin (TRTIC)
anti-TOM20 (FITC)
Compare:
endogenous PINK1 induction
(Parental + CCCP) versus
measured PINK1 input threshold
Untreated (Parental)
CCCP 3h (Parental)
Rapalog 3h (synthetic circuit)
Measured
input threshold
Counts (proportion)
anti-Pink1mito intensity (AFU/px; PINK1mito concentration)
B
CMPD39 (1uM)
inhibitior of USP30
D
Time of Parkinmito recruitment (h)
Mean PINK1mito concentration (AFU/pixel)
Vehicle
CMDP39
Input threshold
Activation delay hyperbola
C
Vehicle ( )
CMPD39 ( )
Max Parkinmito loc. (unitless)
73.2
68.9
y=281/(x-73.2) R2 = 0.878
y=238/(x-68.9) R2 = 0.884
Time of Parkinmito recruitment (h)
Mean PINK1mito concentration (AFU/pixe)
E
Input threshold (AFU/pixel)
Delay multiplier (h*AFU/pixel)
Vehicle
CMPD39
*
***

Figure S6. Additional characterization of the PINK1/Parkin synthetic circuit, related to Figure 1 and 2. (A) Endogenous $PINK1^{mito}$ levels are much lower than that of the synthetic circuit. Comparison of endogenous $PINK1^{mito}$ levels following CCCP treatment versus ectopically expressed $PINK1^{mito}$ levels following rapalog treatment for single cells (methods). The measured PINK1 input threshold is noted for reference. Schematic: experimental approach. FPs: fluorescent proteins. Imaging channels noted. Schematic bar lengths not to scale. **(B)** Chemical structure of the USP30 inhibitor, CMPD39. **(C)** Quantification of circuit behaviors from live-cell data. CMPD39 or vehicle treatment begun 2 hours prior to rapalog treatment (methods). Points: individual cells, colored by local point density. Data from four experimental replicates was pooled. **(D)** Threshold and hyperbolas from (C), overlaid. **(E)** Bootstrap statistical analysis of input threshold and delay scaler values for data in (C). Mean, 95% confidence intervals, and statistical significance calculated by bootstrap analysis (B=10,000). Bonferroni multiple comparison adjustment. *$p<0.05$; ***$p<0.001$.